A pilot toxicology study of single-walled carbon nanotubes in a small sample of mice

MEIKE L. SCHIPPER[1], NOZOMI NAKAYAMA-RATCHFORD[2], CORRINE R. DAVIS[3], NADINE WONG SHI KAM[2], PAULINE CHU[3], ZHUANG LIU[2], XIAOMING SUN[2], HONGJIE DAI[2] AND SANJIV S. GAMBHIR[1]*

[1]Molecular Imaging Program at Stanford (MIPS), Department of Radiology and Bio-X Program, Palo Alto, California 94305-5427, USA
[2]Department of Chemistry, Palo Alto, California 94305-5427, USA
[3]Department of Comparative Medicine, Stanford University, Palo Alto, California 94305-5427, USA
*e-mail: sgambhir@stanford.edu

Published online: 30 March 2008; doi:10.1038/nnano.2008.68

Single-walled carbon nanotubes are currently under evaluation in biomedical applications, including *in vivo* delivery[1–3] of drugs[4], proteins, peptides[5–7] and nucleic acids[8,9] (for gene transfer[10] or gene silencing[11]), *in vivo* tumour imaging[12] and tumour targeting of single-walled carbon nanotubes as an anti-neoplastic treatment[5]. However, concerns about the potential toxicity of single-walled carbon nanotubes have been raised[13,14]. Here we examine the acute and chronic toxicity of functionalized single-walled carbon nanotubes when injected into the bloodstream of mice. Survival, clinical and laboratory parameters reveal no evidence of toxicity over 4 months. Upon killing, careful necropsy and tissue histology show age-related changes only. Histology and Raman microscopic mapping demonstrate that functionalized single-walled carbon nanotubes persisted within liver and spleen macrophages for 4 months without apparent toxicity. Although this is a preliminary study with a small group of animals, our results encourage further confirmation studies with larger groups of animals.

Cell culture studies have shown evidence of cytotoxicity and oxidative stress induced by single-walled carbon nanotubes[15–20] (SWNTs), with water-soluble, functionalized, pristine nanotubes being less cytotoxic than non-functionalized or oxidized tubes[18,21,22]. Following intratracheal instillation of SWNTs, a dose-dependent inflammation and formation of small nodules, known as epitheloid granuloma, has been seen in the lungs of animals[23–25]. However, little is known about the acute and chronic toxicity of SWNTs when they enter the bloodstream. In the presence of high concentrations of SWNTs, ferric chloride activates platelets, leading to the formation of blood clots[26]. However, biodistribution and imaging studies of SWNTs without ferric chloride[12,27–29] have shown no immediate toxicity of low doses of intravenously injected SWNT, implying that platelet function and blood clot formation is normal in the absence of ferric chloride.

In this study, non-covalently pegylated SWNTs (SWNT PEG) were tested as a 'least toxic scenario', and oxidized, covalently functionalized nanotubes (SWNT O PEG) were used as a 'most toxic scenario'. This was based on the results of cell culture studies that showed water-soluble, functionalized, pristine nanotubes to be less cytotoxic than non-functionalized or oxidized tubes[18,21,22]. The dose was determined by the solubility limit of the constructs and the maximum volume that can be injected into mice without causing potential cardiovascular effects. Concentrations between 10- and 100-fold lower than those used in the present study are generally sufficient in biomedical applications[8,27,28]. Control animals were injected with saline. The subjects were 8- to 12-week-old nude mice, the most prevalent animal model for tumour research, which is our main research interest. The T-cell deficiency of nude mice may, however, affect some results, such as granuloma development, and further studies in other mouse strains are needed. Unrelated pathology observed within the entire colony included bite wounds among male mice while establishing dominance patterns, and orthokeratotic dermatitis, a sporadic skin infection in nude mice caused by corynebacteria.

Upon injection, and throughout the entire study, no unusual behaviour or differences between groups were observed, including vocalizations, laboured breathing, difficulties moving, hunching or unusual interactions with cage mates. No ECG changes or significant blood pressure changes were observed during or immediately following injection (see Supplementary Information, Fig. S1, for ECG results, and Table S1 for blood pressure data), alleviating concerns about potential cardiovascular toxicity based on reports of acute cardiovascular effects following inhalation of fine particulate matter (FPM) such as combustion-generated carbon nanoparticles[30]. Differences in formulation and route of administration in previous inhalation studies likely explain the absence of cardiotoxic effects with intravenously injected SWNT O PEG and SWNT PEG.

Same-sex mice were housed together in groups of five; each group contained one treated mouse and four untreated mice, which were not part of this or any other study. The constant group size was chosen to avoid the effects of group size (such as activity level and body weight) on our measured parameters. All mice in the study survived except for one. At 19 days after injection of SWNT O PEG, a mouse that, up to that point, had

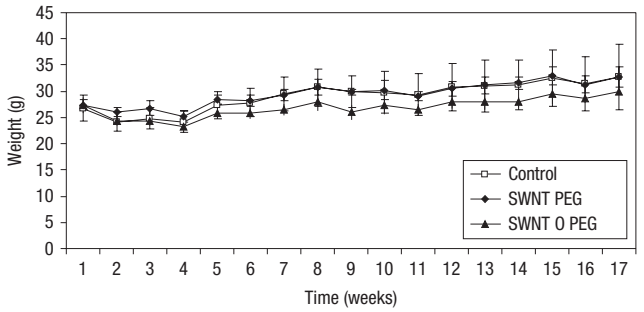

Figure 1 Body weight of nude mice following injection of SWNTs. Mean and standard deviation of body weight of nude mice injected intravenously with SWNT PEG (black diamonds, $n = 4$), SWNT O PEG (black triangles, $n = 4/3$) or PBS control (white squares, $n = 4$) show no statistically significant differences over a period of 4 months.

shown no sign of weakness or illness, received a leaky water bottle, which ran out and soaked the bedding. By the time the accident was discovered, all mice in the cage (treated and untreated) were dead or moribund.

Overall, body weight increased slightly but insignificantly throughout the study in all groups as mice matured (Fig. 1). Blood counts did not differ significantly between groups, nor did they change significantly throughout the study, with the exception of mean corpuscular volume and mean corpuscular haemoglobin, which were higher in both treated groups. Further study is warranted to investigate this finding. There was considerable spread in white blood cell and neutrophil counts, likely resulting from the above-mentioned skin infections (Fig. 2). Blood chemistries were within normal ranges and did not differ significantly between groups at the time of killing (Fig. 2; see also Supplementary Information, Table S2). Careful and extensive necropsy did not reveal gross abnormalities or abnormal organ weights. Age-related changes were noted on histology in both control and treated mice (see Supplementary Information, Table S3). Pertinently, no significant inflammatory lesions were found in treated or control mice, in contrast with reports of interstitial inflammation and epitheloid granuloma formation following intratracheal instillation of unmodified, hydrophobic SWNTs in other studies[23–25]. The route of administration and presence of hydrophilic surface modification, such as the PEG used here, are likely to change biodistribution and affect toxicity. Intravenously injected SWNTs are taken up by liver and spleen[12] or excreted rapidly through the kidneys[28,29]. The biodistribution following intratracheal instillation is unknown, but granuloma formation implies uptake by lung macrophages, with prolonged presence in the organism, and thus increased toxic potential.

Previously, FPM has been linked to increased risk of stroke and myocardial infarction (heart attack). We found no evidence of increased cardiovascular pathology in the treated animals, including thrombosis, atherosclerosis, stroke or myocardial infarction. Again, route of administration and formulation likely explain the difference. However, mice as a species are less prone to developing atherosclerotic changes than primates, and subtle pro-atherogenic effects might be missed unless an atherogenic mouse model were to be used. One mouse had inflammation in the spleen, the wall of the right atrium, lung artery and liver tissue, likely in a setting of bacteremia (bacteria in the bloodstream).

All SWNTs persisted within the body for four months after injection. All treated mice had small amounts of a distinctive, finely granular brown-black pigment throughout the liver tissue, which is likely to be the SWNTs. The pigments were localized within liver macrophages (immune cells that are responsible for 'eating' foreign materials such as viruses, bacteria or dust particles) (Fig. 3b,c), as demonstrated by the F4/80 stain—a monoclonal antibody that recognizes the mouse macrophage antigen (data not shown). Normal liver macrophages typically showed no evidence of cell injury, and normally contained a small amount of golden-brown pigment, which was darker and more finely granular than haemosiderin, a common age-related golden-brown pigment from haemoglobin breakdown found in many tissues. Haemosiderin was observed throughout the spleen (but not in the liver), and in particular in spleen macrophages (Fig. 3e,f), and was confirmed to be a haem-based pigment by Perl's iron stain (not shown). However, small amounts of the finely granular brown-black pigment that we believe are SWNTs could conceivably be obfuscated by the much larger amounts of haemosiderin in splenic macrophages.

In vitro Raman spectra of SWNT PEG and SWNT O PEG preparations in phosphate buffered saline (PBS) reveal a distinct signal peak around 1,590 cm^{-1} (G-peak; Fig. 4c). Equal concentrations of SWNT O PEG gave lower signals than SWNT PEG due to covalent damage to the carbon atom networks in SWNT O PEG sidewalls from the oxidation process. Raman microscopy of paraffin-embedded, glass-mounted mouse tissue sections revealed focal increases in Raman G-peak signal in liver and spleen of SWNT PEG mice four months after injection. The signal was stronger in liver than in spleen. SWNT O PEG mice showed a weak signal in some foci in the liver and spleen. No signal was detected in organs of control animals. Raster area sampling and two-dimensional mapping of Raman spectra showed focal increases in Raman signal, consistent with a macrophage location for the SWNT PEG in SWNT PEG animals (Fig. 5b,e). In SWNT O PEG animals, foci of increased Raman signal were seen in the liver, but spleen signal was not unequivocally focal, being very weak (Fig. 5c,f). Predictably, no foci of increased Raman signal were observed in control animals (Fig. 5a,d). Although we have previously shown SWNT uptake in the liver upon intravenous injection[22], this is the first time that Kupffer cell localization has been confirmed, and that long-term persistence of functionalized SWNTs within liver macrophages without relevant pathology has been shown.

Although SWNT O PEG animals displayed greater amounts of pigment in their Kupffer cells, the Raman signal was less intense than in SWNT PEG mice, likely due to the inherently weaker Raman signal of oxidized SWNTs (Fig. 4c). Raman mapping should be considered a semi-quantitative method, where a lower signal can be caused by lower levels of SWNTs or by increased damage to carbon hexagon structures. The absence of a focal signal in the spleen of the SWNT O PEG mice could be a result of the absence of SWNT O PEG, or of a signal of below background levels due to the inherently weaker signal.

This study demonstrates the first systematic toxicity evaluation of functionalized SWNTs following intravenous injection. Single administrations of high doses did not lead to acute or chronic toxicity in nude mice, but some changes in red blood cells were observed. Because of the small number of animals, our findings must be considered a pilot study. The power of the study to detect small differences between groups is statistically limited by the small number of animals. If a larger number of animals were used, the power to detect small differences between the treatment groups in our study would be greater and statistically more meaningful. Although more extensive series are needed to confirm our results and show equivalence in other mouse strains, they do encourage further exploration of functionalized SWNTs in biomedical applications in living animals.

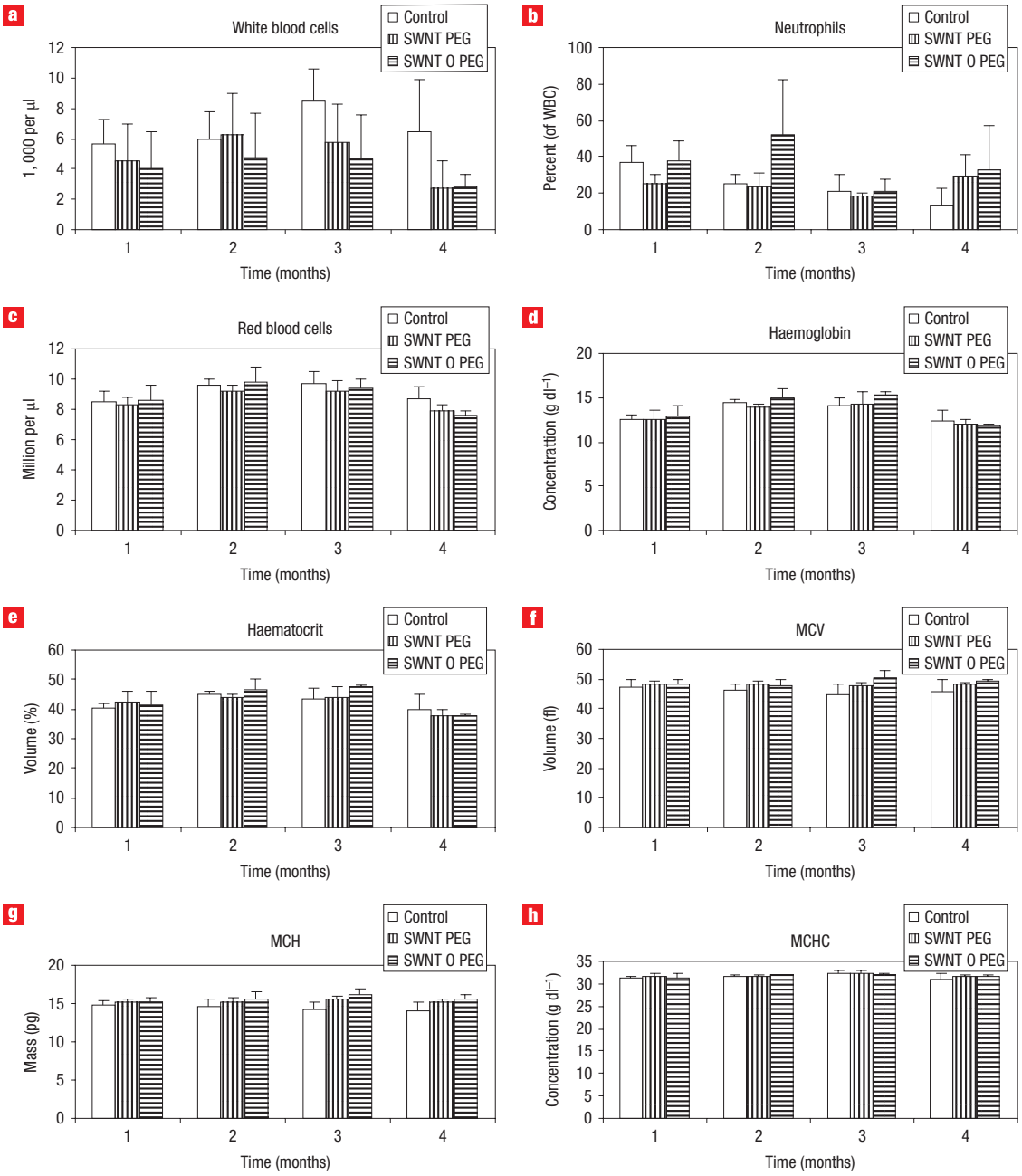

Figure 2 Complete blood counts of nude mice following injection of SWNTs. a–h, Mean and standard deviation of white blood cell (WBC) numbers (**a**), percentage of neutrophils among white blood cells (**b**), red blood cell numbers (**c**), haemoglobin concentration (**d**), haematocrit (**e**), mean corpuscular volume (MCV) (**f**), mean corpuscular haemoglobin (MCH) (**g**), or mean corpuscular haemoglobin concentration (MCHC) (**h**) of nude mice ($n = 4$ per group), all plotted over a period of 4 months following injection of SWNT PEG (vertical stripes), SWNT O PEG (horizontal stripes) or PBS control (white). No statistically significant changes were observed between groups or over time throughout the duration of the study.

METHODS

For non-covalent functionalization of SWNTs (SWNT PEG), 1 mM of NHS-PEG-BOC-3400 (Nektar Therapeutics) was added to 0.36 mM PL-PEG-NH_2 (1,2-distearoyl-*sn*-glycero-3-phosphoethanolamine-*N*-[amino(polyethylene glycol)2000], Avanti Polar Lipids) in 100 mM phosphate buffer at pH 7.5. The resulting PL-PEG solution was sonicated with SWNTs (HiPco, CNI,) for ~1 h and centrifuged at ~25,000*g* for 6 h. The SWNT PEG supernatant was collected, centrifuge filtered (Millipore Microcon 100 kDa, Millipore), and suspended in (pH 7.4). Concentration was determined by UV-visible-NIR spectroscopy (Cary 6000i; $\varepsilon = 7.9 \times 10^6\ M^{-1}\ cm^{-1}$ at 808 nm). For covalent functionalization (SWNT O PEG), the SWNTs were refluxed and oxidized in 2.5 M nitric acid for 24 h, filtered though a polycarbonate filter membrane (200 nm, Whatman), washed, resuspended, centrifuged and concentrated as above. For PEG–SWNT O conjugation, 100 nM of SWNT O was incubated with 1 mM of O,O′-*bis*(2-aminoethyl)polyethylene glycol, ($M_w = 10{,}000$) and 2 mM of *N*-ethyl-*N*′-(3-dimethylaminopropyl)carbodiimide hydrochloride (Sigma-Aldrich) for 2 h, and filtered through a polycarbonate filter membrane, resuspended, centrifuged, and concentrated to a 1 µM solution as above.

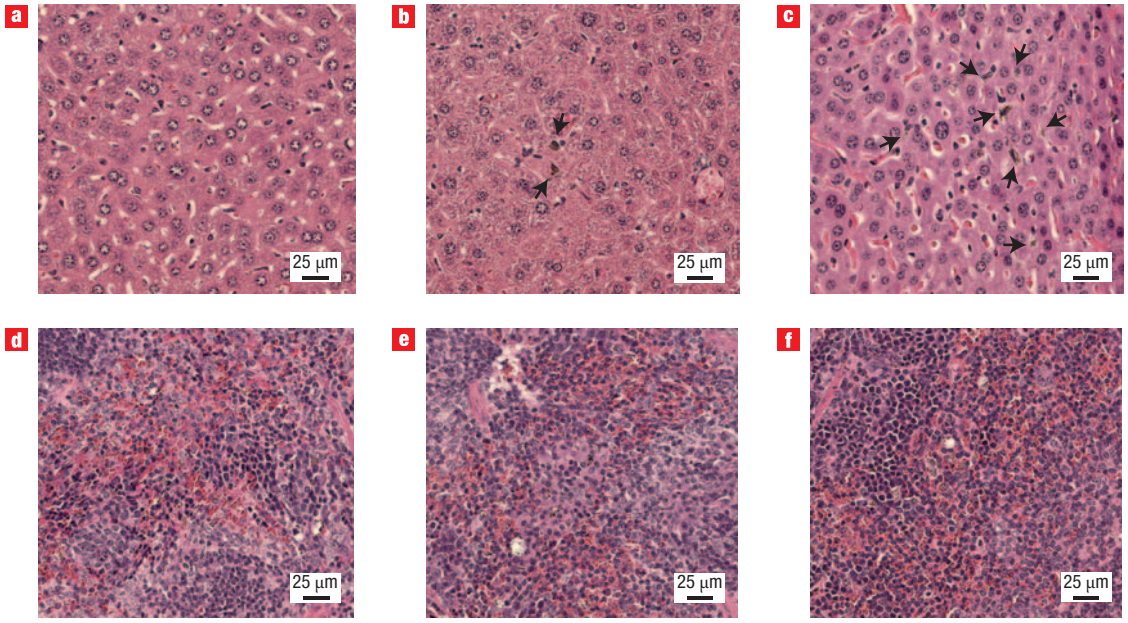

Figure 3 Liver and spleen histology. a–f, Haematoxylin and eosin stains of liver (**a–c**) and spleen (**d–f**) tissues of mice injected with PBS (**a**,**d**), SWNT PEG (**b**,**e**) or SWNT O PEG (**c**,**f**). Finely granular brown-black pigments were seen in sinusoidal liver cells of SWNT PEG (**b**, arrows) and SWNT O PEG (**c**, arrows), as well as a golden-brown pigment in spleen macrophages of SWNT PEG and SWNT O PEG (**e**,**f**), without signs of cellular or tissue damage.

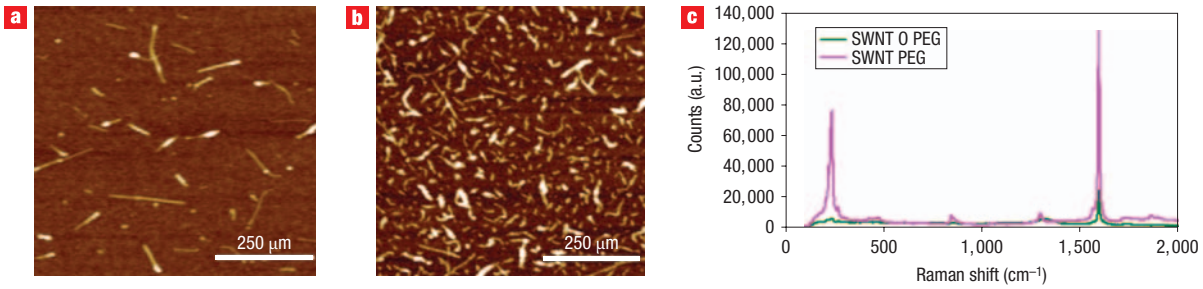

Figure 4 AFM images and Raman spectra of SWNTs. a,**b**, AFM images of SWNT PEG (**a**) and SWNT O PEG (**b**), showing absence of aggregates. **c**, Raman spectra of SWNT PEG and SWNT O PEG in water showing a distinct peak at 1,590 cm^{-1} (G-band), corresponding to the graphitic stretch of SWNT. SWNT O PEG samples display lower peaks as a result of covalent damage to the sidewalls.

For atomic force microscopy (AFM), ~20 μl of 1 μM SWNT suspension was incubated on a silicon substrate for ~15 min, rinsed briefly with water, and air dried. Non-covalently pegylated (M_w = 5,400) Hipco nanotubes measured 1–5 nm in diameter and 100–300 μm in length; oxidized SWNTs were 50–200 nm in length (Fig. 4). Both were well soluble in water at concentrations greater than 3 mg ml^{-1}. No aggregation was observed in PBS or cell culture media for more than one month[12].

Animal experiments were conducted in compliance with all relevant guidelines and regulations, and were approved by the Stanford Administrative Panel on Laboratory Animal Care (APLAC). Eight- to twelve-week-old nude mice (Charles Rivers Laboratories) were housed in groups of five in standard cages with free access to food and water and a 12-h light/dark cycle. Mice were housed in same-sex groups, together with untreated nude mice, to make groups of five. We chose to maintain a constant group size of five in order to avoid effects of group size on our measured parameters (group size will affect parameters such as activity level and body weight). We also distributed treated mice between cages in order to prevent worst-case scenarios such as a simultaneous loss of five study mice due to accident. The mice that were used to fill the cages up to the desired group size of five were all untreated nude mice that were not used for any other experiments for the duration of the study. They originated from the same social group as the study mouse to minimize social stress. Animals were observed daily and weighed weekly, and upon killing.

Two female and two male mice each were randomly assigned to three test groups, and injected intravenously with either PBS, 1 μM of SWNT PEG or 1 μM of SWNT O PEG, under isoflurane anaesthesia. Control and SWNT PEG animals were injected twice with 100-μl sterile PBS (or SWNT PEG, respectively) on days 0 and 7. SWNT O PEG mice were injected once with 100 μl of SWNT O PEG in sterile PBS, and once with 100 μl of sterile PBS at days 0 and 7, due to the limited availability of the compound. The total mass of injected compound was 151 mg of SWNT PEG and 47 mg of SWNT O PEG (see discussion in Supplementary Information).

Blood pressure was measured using a tail cuff device (Coda 6, Kent Scientific Corporation) immediately before and after injection. ECG was measured subcutaneously 5 min before injection, throughout injection, and continuing for 10 min after injection. For complete blood counts (CBC), 75 μl of blood was collected by retro-orbital bleed every four weeks through a heparin-coated glass capillary. Animals were killed by cervical dislocation

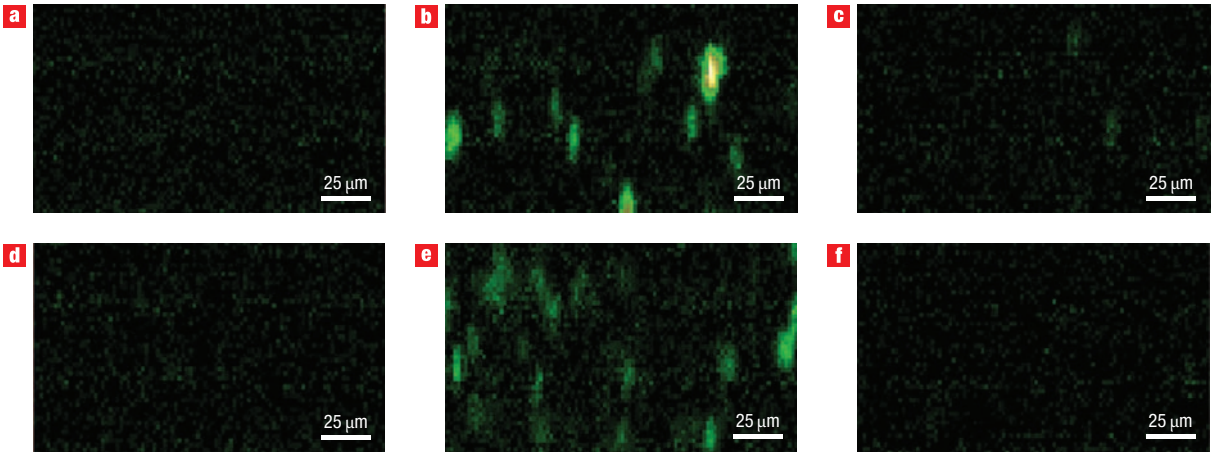

Figure 5 Micro-Raman mapping of paraffin-embedded mouse tissues. a–f, Two-dimensional sampling and mapping of Raman spectra in liver (**a–c**) and spleen (**d–f**) tissues of mice injected with PBS (**a**,**d**), SWNT PEG (**b**,**e**) or SWNT O PEG (**c**,**f**). Focal increases in the Raman signal were consistent with intracellular persistence of SWNT PEG and SWNT O PEG in macrophages 4 months after intravenous injection.

12 weeks after injection. One mouse was killed prematurely 3 weeks after injection due to a water bottle accident. Immediately afterwards, 1 ml of blood was collected by cardiac puncture, and CBC and chemistry panel determinations were performed at the Veterinary Service Center of the Department of Comparative Medicine, Stanford University. A full gross necropsy examination was performed. The weight of liver and spleen, as well as of any unusually sized organs, was recorded. Tissues were fixed in 10% neutral buffered formalin, processed routinely into paraffin, and 4-μm sections were stained with haematoxylin and eosin (Histotec Laboratories). Liver, spleen, kidney, heart, salivary glands, mandibular lymph node, lung, trachea, tongue, oesophagus, gastrointestinal tract, pancreas, mesenteric lymph node, ovary, uterus, urinary bladder, nasal epithelium, eyes, brain, spinal cord, bone, bone marrow, skeletal muscle and skin were examined by light microscopy by a blinded mouse veterinary pathologist. Perl's iron stain, Period Acid Schiff's stain, and immunohistochemistry for F4/80 macrophage-specific membrane marker (rat anti-mouse monoclonal antibody, Serotec) were used on the liver and spleen as appropriate.

For micro-Raman mapping, slides were focused in a Raman microscope (Renishaw) at ×20 magnification and excited with a 785-nm laser (100 mW). Images were obtained by scanning a 200 μm × 124 μm area in 2 μm × 2.64 μm steps, and collecting the Raman spectrum at each spot (Renishaw, 2-s integration time), and plotting the integral of the area under the curve from 1,570–1,610 cm^{-1} (G-peak characteristic of SWNTs) in the corresponding spot to form the area image.

Because repeated-measures ANOVA is not robust for small unbalanced samples, separate unpaired Wilcoxon tests were used to compare SWNT O PEG with Control and SWNT PEG with Control. The tests were either exact, or used permutation samples of 1,000,000. For blood counts, stratified Wilcoxon tests of group on each variable, stratified by week, were performed. For body weight, stratified Wilcoxon tests of group on weight, stratified by week, sex, and both week and sex were performed, as well as tests of sex on weight, stratified by week. For post-mortem organ weight, simple Wilcoxon tests of group on weight were performed. For blood pressure, simple Wilcoxon tests of group on the post–pre differences in blood pressure were performed. A value of $P < 0.05$ was considered statistically significant. It should be noted that as this is a pilot study the power relative to the detectable effect size of the study is limited. For a minimum power of 0.80 (assuming a normal distribution and no need for stratification) then the blood pressure and organ weight tests could detect a difference of only two standard deviations, the blood chemistry tests hadthe power to detect differences of one standard deviation, and the body weight test could detect a difference of half a standard deviation.

Received 15 January 2008; accepted 29 February 2008; published 30 March 2008.

References

1. Bianco, A. *et al.* Biomedical applications of functionalised carbon nanotubes. *Chem. Commun.* 571–577 (2005).
2. Bianco, A., Kostarelos, K. & Prato, M. Applications of carbon nanotubes in drug delivery. *Curr. Opin. Chem. Biol.* **9,** 674–679 (2005).
3. Klumpp, C. *et al.* Functionalized carbon nanotubes as emerging nanovectors for the delivery of therapeutics. *Biochim. Biophys. Acta* **1758,** 404–412 (2006).
4. Wu, W. *et al.* Targeted delivery of amphotericin B to cells by using functionalized carbon nanotubes. *Angew. Chem. Int. Edn* **44,** 6358–6362 (2005).
5. Kam, N. W. *et al.* Carbon nanotubes as multifunctional biological transporters and near-infrared agents for selective cancer cell destruction. *Proc. Natl Acad. Sci. USA* **102,** 11600–11605 (2005).
6. Kam, N. W., Liu, Z. & Dai, H. Carbon nanotubes as intracellular transporters for proteins and DNA: an investigation of the uptake mechanism and pathway. *Angew. Chem. Int. Edn* **45,** 577–581 (2006).
7. Pantarotto, D. *et al.* Translocation of bioactive peptides across cell membranes by carbon nanotubes. *Chem. Commun.* 16–17 (2004).
8. Pantarotto, D. *et al.* Functionalized carbon nanotubes for plasmid DNA gene delivery. *Angew. Chem. Int. Edn* **43,** 5242–5246 (2004).
9. Singh, R. *et al.* Binding and condensation of plasmid DNA onto functionalized carbon nanotubes: toward the construction of nanotube-based gene delivery vectors. *J. Am. Chem. Soc.* **127,** 4388–4396 (2005).
10. Liu, Y. *et al.* Polyethylenimine-grafted multiwalled carbon nanotubes for secure noncovalent immobilization and efficient delivery of DNA. *Angew. Chem. Int. Edn* **44,** 4782–4785 (2005).
11. Kam, N. W., Liu, Z. & Dai, H. Functionalization of carbon nanotubes via cleavable disulfide bonds for efficient intracellular delivery of siRNA and potent gene silencing. *J. Am. Chem. Soc.* **127,** 12492–12493 (2005).
12. Liu, Z. *et al. In vivo* biodistribution and highly efficient tumour targeting of carbon nanotubes in mice. *Nature Nanotech.* **2,** 47–52 (2007).
13. Lison, D. & Muller, J. Lung and systemic responses to carbon nanotubes (CNT) in mice. *Toxicol. Sci.* **101,** 179–180 (2008).
14. Mitchell, L. A. *et al.* Pulmonary and systemic immune response to inhaled multiwalled carbon nanotubes. *Toxicol. Sci.* **100,** 203–214 (2007).
15. Monteiro-Riviere, N. A. *et al.* Multi-walled carbon nanotube interactions with human epidermal keratinocytes. *Toxicol. Lett.* **155,** 377–384 (2005).
16. Shvedova, A. A. *et al.* Exposure to carbon nanotube material: assessment of nanotube cytotoxicity using human keratinocyte cells. *J. Toxicol. Environ. Health A* **66,** 1909–1926 (2003).
17. Cui, D. *et al.* Effect of single wall carbon nanotubes on human HEK293 cells. *Toxicol. Lett.* **155,** 73–85 (2005).
18. Bottini, M. *et al.* Multi-walled carbon nanotubes induce T lymphocyte apoptosis. *Toxicol. Lett.* **160,** 121–126 (2006).
19. Kagan, V. E. *et al.* Direct and indirect effects of single walled carbon nanotubes on RAW 264.7 macrophages: Role of iron. *Toxicol. Lett.* **165,** 88–100 (2006).
20. Tian, F. *et al.* Cytotoxicity of single-wall carbon nanotubes on human fibroblasts. *Toxicol. In Vitro* **20(7)** 1202–1212 (2006).
21. Sayes, C. M. *et al.* Functionalization density dependence of single-walled carbon nanotubes cytotoxicity *in vitro. Toxicol. Lett.* **161,** 135–142 (2006).
22. Magrez, A. *et al.* Cellular toxicity of carbon-based nanomaterials. *Nano Lett.* **6,** 1121–1125 (2006).
23. Shvedova, A. A. *et al.* Unusual inflammatory and fibrogenic pulmonary responses to single-walled carbon nanotubes in mice. *Am. J. Physiol. Lung Cell Mol. Physiol.* **289,** L698–L708 (2005).
24. Lam, C. W. *et al.* Pulmonary toxicity of single-wall carbon nanotubes in mice 7 and 90 days after intratracheal instillation. *Toxicol. Sci.* **77,** 126–134 (2004).
25. Warheit, D. B. *et al.* Comparative pulmonary toxicity assessment of single-wall carbon nanotubes in rats. *Toxicol. Sci.* **77,** 117–125 (2004).
26. Radomski, A. *et al.* Nanoparticle-induced platelet aggregation and vascular thrombosis. *Br. J. Pharmacol.* **146,** 882–893 (2005).
27. Wang, H. *et al.* Biodistribution of carbon single-wall carbon nanotubes in mice. *J. Nanosci. Nanotechnol.* **4,** 1019–1024 (2004).
28. Singh, R. *et al.* Tissue biodistribution and blood clearance rates of intravenously administered carbon nanotube radiotracers. *Proc. Natl Acad. Sci. USA* **103,** 3357–3362 (2006).

29. Cherukuri, P. *et al*. Near-infrared fluorescence microscopy of single-walled carbon nanotubes in phagocytic cells. *J. Am. Chem. Soc.* **126,** 15638–15639 (2004).
30. Urch, B. *et al*. Acute blood pressure responses in healthy adults during controlled air pollution exposures. *Environ. Health Perspect.* **113,** 1052–1055 (2005).

Acknowledgements

This study was supported in part by grants from the National Cancer Institute Center for Cancer Nanotechnology Excellence (CCNE) U54 CA119367 (S.S.G.) and In vivo Cellular and Molecular Imaging Center (ICMIC) P50 CA114747 (S.S.G.).

Correspondence and requests for materials should be addressed to S.S.G.
Supplementary information accompanies this paper on www.nature.com/naturenanotechnology.

Author contributions

M.L.S. and S.S.G. conceived and designed the experiments. M.L.S. performed the experiments. M.L.S. and S.S.G. analysed the data. N.N.R., C.R.D., N.W.S.K., P.C., Z.L., X.S. and H.D. contributed materials and analysis tools. M.L.S. and S.S.G. co-wrote the paper. All authors discussed the results and commented on the manuscript.